

# MORPH-U: Multi-Objective Resilient Motion Planning for V2X-Enabled Autonomous Driving in High-Uncertainty Environments via Simulation

Shih-Yu Lai  
National Taiwan University  
Taipei, Taiwan  
akinesia112@gmail.com

**Abstract**—V2X can warn an autonomous vehicle about hazards beyond line-of-sight, but it also brings uncertainty: messages may be delayed, dropped, or even forged. Meanwhile, map knowledge may change during a trip, forcing the vehicle to replan under tight real-time budgets. This paper studies how to make motion planning and low-level control robust to such uncertain, event-driven updates. We present MORPH-U, a CARLA-based closed-loop stack that fuses LiDAR/radar/camera with V2X (CAM/DENM) into a Local Dynamic Map (LDM) and triggers Hybrid-A\* replanning when validated hazards or map changes affect the planned route. We expose the planning/control trade-offs via a multi-objective formulation over tracking error, safety margin (minimum TTC), responsiveness, and smoothness, and select operating points using Pareto-frontier analysis. To avoid unsafe replanning from faulty V2X triggers, MORPH-U adds a lightweight Byzantine-inspired acceptance gate that combines a quorum rule with an on-board sensor veto. Experiments in dynamic CARLA scenarios show that V2X-augmented LDM improves downstream safety, Pareto tuning provides controllable accuracy-comfort trade-offs, and the gate prevents replanning under saturated false-DENM injection ( $p_{\text{attack}}=1.0$ ).

**Index Terms**—V2X Communication, Motion Planning, Multi-Objective Optimization, Event-Driven Replanning, Resilient Autonomous Driving, CARLA Simulator.

## I. INTRODUCTION

V2X promises earlier hazard awareness than on-board sensing alone, but in practice V2X inputs are uncertain: messages can arrive late, be lost, or be incorrect under realistic wireless conditions and dynamic traffic [1]–[3]. For a vehicle operating near safety margins, such uncertainty directly affects *when* to replan and *how* aggressively to control. In addition, road knowledge can change during execution (e.g., closures or topology updates), which may invalidate the current route and require replanning within a fixed control cycle [4].

While prior work studies V2X cooperation [1], [2], uncertainty-aware perception [5], and simulation toolchains [6], [7], fewer studies connect them *in a closed loop* with measurable planning/control trade-offs under event-driven V2X/map updates, where safety, tracking, and smoothness are inherently competing. We present MORPH-U, a CARLA-based vehicle-side pipeline that (i) fuses LiDAR/radar/camera with V2X CAM/DENM into a Local Dynamic Map (LDM), (ii) runs Hybrid-A\*

planning with event-driven replanning, and (iii) executes trajectories using Pure Pursuit and PID control [6]. On top of this loop, we add two mechanisms that target the above uncertainties: a multi-objective Pareto analysis for selecting operating points across tracking, safety, responsiveness, and smoothness [8], [9]; and a lightweight Byzantine-inspired acceptance gate that filters V2X-triggered replanning events before they affect the vehicle [10], [11].

Our contributions are:

- 1) A V2X-augmented LDM that integrates CAM/DENM with on-board sensing and supports closed-loop planning under uncertain external inputs [1], [2], [5].
- 2) An event-driven Hybrid-A\* replanning loop in CARLA that reacts to validated hazards and map changes during execution [4], [6].
- 3) A multi-objective formulation and Pareto-frontier analysis that makes safety-tracking-smoothness trade-offs explicit and selectable [8], [9].
- 4) A Byzantine-inspired acceptance gate for V2X-triggered replanning, evaluated under injected false-event attacks [10], [11].

We position MORPH-U as an *integration* contribution: Hybrid-A\*, Pure Pursuit, PID, and quorum-style filtering are individually standard. The novelty lies in (i) routing CAM/DENM through a probabilistically-fused LDM that is the *sole* planner interface, enabling clean ablations; (ii) treating planner re-entry as an explicit, gated event rather than continuous re-optimization; and (iii) reporting V2X’s downstream effect on a *measured* Pareto frontier rather than at hand-tuned points.

We evaluate MORPH-U in CARLA urban intersections under both multi-vehicle traffic and single-vehicle route-following setups (Fig. 1), covering baseline tracking (S1), V2X hazard response (S2), update-induced rerouting (S3), and faulty-trigger attacks (S4).

## II. RELATED WORK

### A. V2X-augmented perception under uncertainty

V2X has been widely studied as a mechanism to extend perception beyond line-of-sight through cooperative awareness and event-driven safety messages, enabling cooperative



(a) Multi-vehicle urban intersection (S2/S4). (b) Single-vehicle route-following (S1/S3).

Fig. 1. CARLA simulator evaluation setups in MORPH-U. (a) Multi-vehicle urban intersection used for V2X-enabled hazard response and faulty-trigger robustness (S2/S4). (b) Single-vehicle route-following used for baseline tracking and Pareto operating-point selection (S1), and as the backbone setting for update-induced rerouting (S3).

and infrastructure-aided perception in dynamic traffic [1]–[3]. In parallel, uncertainty-aware fusion has long relied on Bayesian and evidential formulations to represent ambiguity and combine heterogeneous sensing sources [5], [12]–[14]. Learning-based modules further enhance perception and downstream tasks in such pipelines [14], [15]. These works establish that V2X can improve the world model, but they typically stop short of quantifying how such improvements propagate through a closed-loop planner and controller under event-driven updates.

### B. Planning, control, and multi-objective operating points

Search-based planning and classical controllers remain common baselines for closed-loop autonomy, especially when reproducibility and auditable failure modes are required in safety studies [6], [16]. However, in realistic settings, safety, tracking, responsiveness, and smoothness are competing objectives that cannot be optimized simultaneously. Multi-objective optimization offers a principled lens to expose and select operating points via Pareto-optimal sets and quality indicators [8], [9]. Yet, much of the autonomy literature reports results at a small number of hand-tuned configurations, leaving the trade-off structure implicit and making it difficult to compare planning/control behaviors across scenarios with different uncertainty profiles.

### C. Resilience to faulty V2X triggers and map inconsistency

V2X inputs introduce a new failure surface: incorrect or adversarial reports can trigger unsafe braking or replanning, motivating resilience mechanisms grounded in Byzantine reasoning and robust aggregation [10], [11], [17]. Separately, maintaining map consistency for downstream autonomy has been studied through HD map representations and validation/update pipelines, including standards such as OpenDRIVE and related change-handling work [4], [18]–[28]. Simulation and toolchains enable controlled evaluations of such effects in integrated pipelines, including V2X-in-the-loop setups and CARLA-based benchmarking [4], [6], [7], [29]–[32]. However, fewer studies combine (i) V2X-augmented fusion, (ii) event-driven replanning induced by hazards and map changes, (iii) explicit Pareto trade-offs in planning/control, and (iv) resilience gating against faulty triggers *within the same closed-loop stack*. MORPH-U targets this gap by integrating these components and reporting mea-

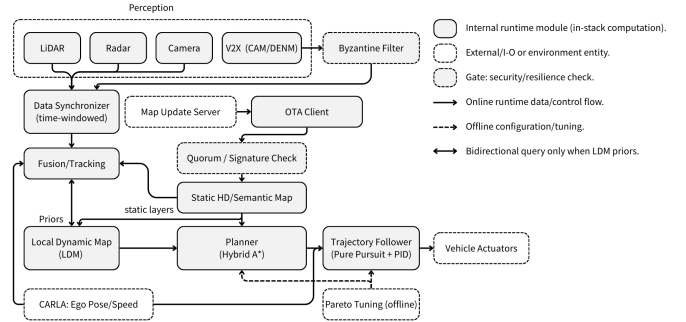


Fig. 2. Closed-loop architecture of MORPH-U. Time-windowed synchronization and fusion populate an ego-centric LDM from on-board sensing and V2X (CAM/DENM). Hybrid-A\* replans when validated events or knowledge changes trigger replanning. Pareto tuning is performed offline to select planning/control operating points. The acceptance gates (V2X and update path) prevent faulty triggers from reaching the planner.

asurable trade-offs and robustness envelopes across scenarios.

## III. SYSTEM AND METHOD

**MORPH-U** is a CARLA-based, vehicle-side closed-loop stack that integrates V2X with multi-sensor perception, search-based planning, and classical control. At each tick, the system (i) buffers on-board sensor frames and V2X messages, (ii) fuses them into a Local Dynamic Map (LDM), (iii) triggers event-driven replanning when hazards or knowledge changes affect the planned route, and (iv) executes the trajectory with a trajectory follower. The design explicitly targets two questions: (a) how V2X improves the fused world model used by the planner, and (b) how to select stable operating points that balance safety, tracking, responsiveness, and smoothness under uncertainty. Figure 2 summarizes the closed-loop execution path and highlights where (i) V2X/map events enter the LDM, (ii) replanning triggers are evaluated, and (iii) the acceptance gate blocks faulty triggers before they affect planning.

### A. V2X-Augmented LDM Fusion

MORPH-U fuses LiDAR/radar/camera detections with V2X messages (CAM/DENM) into an ego-centric LDM that maintains (i) tracked dynamic objects and (ii) discrete hazard/map events relevant to planning. Let  $z_k$  denote an incoming sensor detection or a decoded V2X packet with timestamp  $t_k$ . A synchronizer emits a time-aligned bundle within a sliding window:

$$\mathcal{S}_t = \{(z_k, t_k) \mid t - \tau_{\text{sync}} \leq t_k \leq t\}. \quad (1)$$

A fusion/tracking module associates detections across modalities and updates the LDM state

$$\mathcal{X}_t = \{\mathcal{O}_t, \mathcal{E}_t, \mathcal{M}_t\}, \quad (2)$$

where  $\mathcal{O}_t$  are tracked objects in the ego-local frame,  $\mathcal{E}_t$  are event hypotheses (e.g., DENM hazards, map-change notices), and  $\mathcal{M}_t$  are the active static map layers used for planning. V2X messages are *not* consumed directly: each  $o \in \mathcal{O}_t$  carries an existence belief  $b(o) \in [0, 1]$  updated by Bayesian combination of on-board detection likelihoods and authenticated CAM/DENM reports weighted by source reputation, with on-board sensing acting as a veto when

$\mathcal{L}_{\text{sensor}}$  contradicts a V2X claim within the same spatio-temporal cell. Event hypotheses  $\mathcal{E}_t$  are gated separately by Sec. III-D before they can trigger replanning. This LDM is the sole interface consumed by the planner and controller, enabling controlled ablations (sensors-only vs. sensors+V2X) and deterministic replay.

### B. Planning and Event-Driven Replanning

Given  $\mathcal{X}_t$  and a goal pose, MORPH-U computes a curvature-feasible trajectory using Hybrid-A\* over  $SE(2)$ :

$$|\kappa(s)| \leq \kappa_{\max}, \quad \kappa(s) = \frac{\tan \delta(s)}{L}, \quad (3)$$

with wheelbase  $L$  and steering angle  $\delta(s)$ . Replanning is invoked by three auditable, scenario-controllable triggers: (i) *hazard-on-route*, a validated DENM within a look-ahead horizon on the planned route; (ii) *risk threshold*, a TTC-based predicted-risk excess on the current plan prefix; and (iii) *knowledge change*, an active-map version change after update activation. All triggers route through the gate of Sec. III-D, ensuring that V2X/map signals affect the vehicle only via explicit, logged decisions.

### C. Multi-Objective Formulation and Pareto Operating Points

We expose tunable design variables

$$\theta = \{\text{LA}, K_p, K_i, K_d, \text{replan thresholds, update interval, } \dots\}, \quad (4)$$

and evaluate each configuration on an objective vector

$$\mathbf{J}(\theta) = [J_{\text{trk}}, J_{\text{sfty}}, J_{\text{resp}}, J_{\text{smth}}, J_{\text{eng}}]. \quad (5)$$

We instantiate these objectives as:

$$\begin{aligned} J_{\text{trk}} &:= \text{RMSE}_{\text{lat}}, & J_{\text{sfty}} &:= \max(0, \tau_{\text{sfty}} - \text{TTC}_{\min}), \\ J_{\text{resp}} &:= \alpha t_{\text{v2x}} + \beta t_{\text{upd}}, & J_{\text{smth}} &:= \text{Var}(\delta) + \gamma \text{Var}(\text{thr}), \\ J_{\text{eng}} &:= \text{brake-energy proxy}. \end{aligned} \quad (6)$$

We treat collisions as a hard constraint (discard) or a large penalty. For comparability across objectives, we normalize each objective to  $[0, 1]$  via min-max over the evaluated set:  $\tilde{J}_i = \frac{J_i - J_i^{\min}}{J_i^{\max} - J_i^{\min}}$ . A configuration  $A$  dominates  $B$  if  $\tilde{\mathbf{J}}(A) \preceq \tilde{\mathbf{J}}(B)$  componentwise and strictly smaller in at least one component; the Pareto set  $\mathcal{P}$  is the nondominated subset.

#### a) Knee-point selection.

To select a single operating point for deployment in closed-loop experiments, we choose a knee solution that minimizes distance to the utopia point under zero-collision constraint:

$$\theta^* \in \arg \min_{\theta \in \mathcal{P}} \left\| \tilde{\mathbf{J}}(\theta) \right\|_2 \quad \text{s.t. collisions} = 0. \quad (7)$$

#### b) Hypervolume comparison.

To compare ablations (e.g., sensors-only vs. sensors+V2X; no-update vs. update), we report hypervolume  $\mathcal{H}$  of the Pareto set with respect to a reference point  $\mathbf{r} \succ \max \tilde{\mathbf{J}}$ . Larger  $\mathcal{H}$  indicates a better achievable trade-off surface. (We report measured frontiers and  $\mathcal{H}$  in Sec. V-D.)

### D. Acceptance Gate for Replanning Triggers (Byzantine-Inspired)

**Threat model.** We adopt a *Byzantine-inspired* threat model: V2X reports are authenticated but up to  $f$  of  $n$  stations may fabricate, replay, or equivocate. We do not claim formal Byzantine fault tolerance; instead we use a quorum-with-

sensor-veto rule as a lightweight filter and evaluate it under one saturated injection policy (Sec. V-A, S4).

**Quorum acceptance rule.** For a candidate event  $E$  (e.g., DENM hazard or update notice), let  $\mathcal{M}_t$  be the set of distinct authenticated reports supporting  $E$  within a spatio-temporal window  $(R, \tau_{\text{bft}})$ , and let  $\mathcal{L}_{\text{sensor}}(E)$  be an on-board likelihood (sensor veto). We accept  $E$  only if

$$\sum_{m_i \in \mathcal{M}_t} w_i \mathbf{1}[m_i \text{ supports } E] \geq \Theta \quad \wedge \quad \mathcal{L}_{\text{sensor}}(E) \geq \eta, \quad (8)$$

where  $\Theta$  is chosen to require at least  $2f+1$  distinct corroborations (e.g.,  $\Theta = 2f+1$  with uniform weights), and  $\eta$  enforces the sensor veto. Only accepted events trigger replanning. The gate's guarantees are empirical and limited to the evaluated attack class; coordinated, timing-correlated attacks and sensor-veto bypass are out of scope (Sec. VII).

### Algorithm 1 Pareto Frontier: Nondominated set (fast sweep)

**Input:** normalized objective set  $\{\tilde{\mathbf{J}}(\theta_k)\}_{k=1}^N$   
 $\mathcal{P} \leftarrow \emptyset$   
**for**  $k = 1$  to  $N$  **do**  
  dominated  $\leftarrow$  **false**  
  **for**  $p \in \mathcal{P}$  **do**  
    **if**  $p \preceq \tilde{\mathbf{J}}(\theta_k)$  **then**  
      dominated  $\leftarrow$  **true**; **break**  
    **if**  $\tilde{\mathbf{J}}(\theta_k) \preceq p$  **then**  
      remove  $p$  from  $\mathcal{P}$   
  **if not** dominated **then**  
    add  $\tilde{\mathbf{J}}(\theta_k)$  to  $\mathcal{P}$   
**Output:** Pareto set  $\mathcal{P}$

## IV. IMPLEMENTATION DETAILS

CARLA runs in synchronous mode with fixed time step  $\Delta t$ ; a synchronizer aggregates timestamped sensor/V2X packets within  $\tau_{\text{sync}}$  and emits fused snapshots each tick. Hybrid-A\* operates on the LDM and active map layers, while the trajectory follower combines Pure Pursuit (lateral) and PID (longitudinal) with bounded outputs and anti-windup; look-ahead, gains, and clamps are exposed for Pareto tuning. An update client polls a simulated server for map versions; upon activation, static layers refresh and a replanning trigger is issued at the next tick boundary for consistent state across the control cycle.

TABLE I  
METRICS (UNITS).

Tracking	Lat. RMSE (m), Heading (deg), Completion (%)
Safety	$\text{TTC}_{\min}$ (s), Collisions
Responsiveness	V2X reaction (ms), Update activation (s)
Smoothness	$\text{Var}(\text{steer})$ , $\text{Var}(\text{throttle})$
LDM fidelity	MOTA, MOTP, ID switches
Resilience (S4)	FPR, FNR, Trigger latency (ms)

TABLE II  
PLANNER PERFORMANCE.

Scenario	Success Rate (%)	Avg. CPU Time (ms)	Avg. Path Length (m)
S1 (Baseline)	100.0	28.5 $\pm$ 4.1	150.2
S2 (Hazard)	96.7	35.1 $\pm$ 6.2	158.5
S3 (OTA Reroute)	96.7	38.0 $\pm$ 6.0	165.1
S4 (BFT Attack)	83.3	34.8 $\pm$ 5.9	150.2

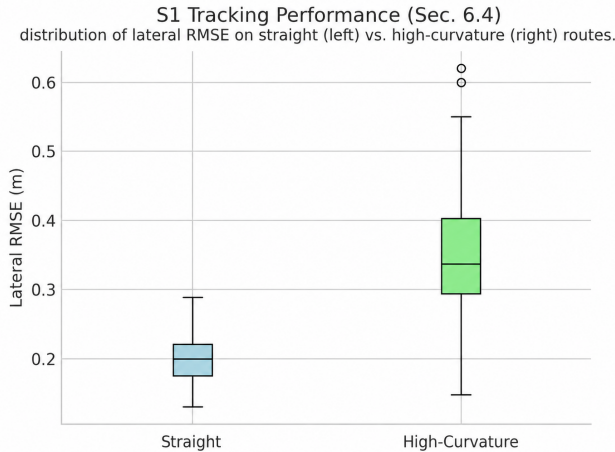


Fig. 3. S1 baseline tracking: distribution of lateral RMSE on *straight* (left) vs. *high-curvature* (right) routes. The widening tail at high curvature is a known Pure Pursuit artifact; rather than masking it via curvature-dependent speed profiling, we expose look-ahead and gains as Pareto variables (Sec. III-C).

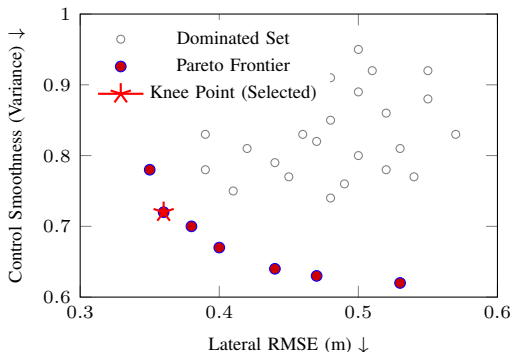


Fig. 4. Pareto frontier (Sec. V-D): Tracking vs. Smoothness ( $N = 60$  configurations). We select the ‘Knee Point’ (red star) for S2-S4 experiments.

## V. EXPERIMENTAL DESIGN

### A. Scenarios

We evaluate four scenarios that isolate V2X benefit, knowledge-change replanning, and resilience:

- **S1 (Tracking):** route following with no V2X and no updates; we vary curvature and speed limits to stress tracking and smoothness.
- **S2 (V2X hazard response):** during motion, we inject a DENM hazard (stationary vehicle / road closure) ahead of the ego vehicle; we compare reactions with and without V2X.
- **S3 (Update-induced reroute):** mid-route, a new map version changes topology (add/remove a segment); the vehicle activates the update and replans to complete the route.
- **S4 (Faulty V2X triggers with a true hazard):** based on S2, we inject a *ground-truth* hazard  $E^*$  (e.g., a stationary vehicle ahead) that is (i) observable by on-board sensing (thus  $\mathcal{L}_{\text{sensor}}(E^*) \geq \eta$ ) and (ii) corroborated by at least  $2f+1$  authenticated *honest* stations within the spatio-temporal window  $(R, \tau_{\text{bit}})$ . In parallel,  $f$  out of  $n$

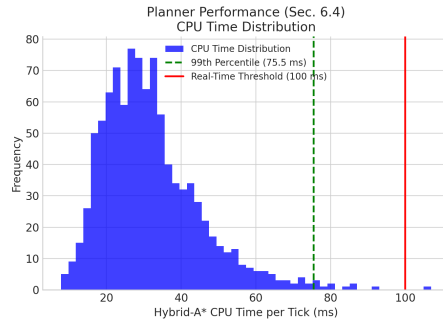


Fig. 5. Hybrid-A\* runtime distribution per tick. The tail remains within the real-time budget in evaluated scenarios.

TABLE III

S2—V2X HAZARD RESPONSE AND LDM FIDELITY. MEAN  $\pm$  SD OVER 30 SEEDS. LDM METRICS ARE COMPUTED AGAINST CARLA GROUND TRUTH, AND MAINLY REFLECT CAM AUGMENTATION.

Config	Lat. RMSE (m) ↓	Min TTC (s) ↑	V2X Lat. (ms) ↓	Collisions ↓	MOTA ↑	MOTP ↑	IDSW ↓
Sensors only	0.42 $\pm$ 0.05	1.30 $\pm$ 0.21	—	5/30	0.78	0.85	22
+ V2X (CAM/DENM)	0.35 $\pm$ 0.04	1.90 $\pm$ 0.18	140 $\pm$ 25	0/30	0.92	0.94	5

stations act as Byzantine attackers and broadcast falsified DENMs at rate  $p_{\text{attack}}$ . We evaluate the acceptance gate under  $n=10$ ,  $f=3$ ,  $p_{\text{attack}}=1.0$ , reporting both FPR (accepting injected false hazards) and FNR (rejecting  $E^*$ , where  $E^*$  is broadcast by  $2f+1$  non-attacking stations and is also present as a CARLA-ground-truth obstacle).

**Planner Analysis:** We profile the Hybrid-A\* planner’s computational performance (success rate, path length, CPU time) across all scenarios (S1-S4) to ensure real-time feasibility (Table II). We also visualize the CPU time distribution (Fig. 5).

### B. Baselines and Ablations

We compare MORPH-U against the following baselines:

- **CARLA Autopilot / BehaviorAgent:** a simulator-provided driving stack as a sanity baseline for route following and hazard scenarios.
- **Sensors-only:** on-board sensing and tracking without any V2X inputs.
- **Sensors + V2X (unfiltered):** V2X CAM/DENM integrated into the LDM without the acceptance gate.

We additionally ablate (i) update on/off in S3 and (ii) controller parameters (look-ahead and PID gains) for Pareto analysis.

### C. Metrics

We report:

- **Tracking:** lateral RMSE (m), heading error (deg), and **completion (%)** (reaching the goal without collision or planner failure).
- **Safety:** minimum time-to-collision  $\text{TTC}_{\text{min}}$  (s) and collision count.
- **Responsiveness:** V2X reaction latency (event timestamp  $\rightarrow$  first decel/steer) and update activation latency (download complete  $\rightarrow$  replan issued).
- **Smoothness:** variance of steering and throttle commands (control effort proxy).

TABLE IV  
S3—OTA-INDUCED REROUTE. MEAN  $\pm$  SD OVER 30 SEEDS.

Config	OTA Act. (s)	Replan Time (ms)	Completion (%)
No-OTA	—	—	72.4 $\pm$ 4.7
OTA enabled	1.1 $\pm$ 0.2	38 $\pm$ 6	96.7 $\pm$ 2.1

TABLE V  
S4—BYZANTINE ATTACK RESPONSE ( $n=10, f=3, p_{\text{ATTACK}}=1.0, N=30$  SEEDS). FNR IS W.R.T. THE INJECTED TRUE HAZARD  $E^*$ .

Config	FPR $\downarrow$	FNR $\downarrow$	Collisions	Completion (%)
Sensors only (Baseline)	N/A	N/A	5/30	83.3 $\pm$ 5.1
V2X (No Filter)	1.00 (30/30)	0.00 (0/30)	0/30	0.0 $\pm$ 0.0
V2X + Quorum Filter	0.00 (0/30)	0.00 (0/30)	0/30	96.7 $\pm$ 2.1

- **LDM fidelity:** MOTA/MOTP and ID switches against CARLA ground truth (reported for sensors-only vs. sensors+V2X CAM).
- **Resilience (S4):** false-positive rate (FPR) for accepting fake hazards, false-negative rate (FNR) for rejecting genuine hazards, and trigger latency under attack.

#### D. Pareto Frontier Protocol

To expose planning/control trade-offs, we perform a grid search over primary controller parameters  $\theta = \{\text{look-ahead}, K_p, K_i, K_d\}$ . We run S1 and S2 for each configuration ( $N=30$  seeds per scenario), compute the objective vector  $\mathbf{J}(\theta)$  (tracking, safety, responsiveness, smoothness; collision as a hard constraint), and extract the nondominated set using Alg. 1. We report measured Pareto frontiers and select a knee-point configuration for subsequent closed-loop evaluations.

## VI. RESULTS

### a) S1: Baseline tracking and control stability.

Figure 3 summarizes lateral RMSE on straight vs. high-curvature routes. The widening tail under curvature is the expected Pure Pursuit-at-speed artifact; rather than absorbing it via curvature-dependent speed profiling, we expose look-ahead  $L_A$  and the gain triple ( $K_p, K_i, K_d$ ) as Pareto variables (Eq. 4) so that the trade-off itself becomes the reported result. Adding a speed profile to  $\theta$  is a natural extension. This motivates the Pareto knee-point selection used in S2–S4.

### b) S2: V2X improves closed-loop safety by enabling earlier hazard response.

Table III shows that adding V2X (CAM/DENM) reduces lateral RMSE from 0.42 m to 0.35 m ( $\approx 16.7\%$ ) and increases  $\text{TTC}_{\min}$  from 1.30 s to 1.90 s ( $\approx 46\%$ ). Collisions drop from 5/30 to 0/30 episodes. The measured V2X reaction latency is  $140 \pm 25$  ms, allowing the controller to initiate braking/steering before the equivalent risk is detectable from on-board sensing alone.

### c) S3: Update-induced replanning restores route feasibility under evolving road knowledge.

Table IV reports that enabling updates improves completion from  $72.4\% \pm 4.7$  to  $96.7\% \pm 2.1$  (+24.3 pp). In the no-update baseline, failures occur after a topology mismatch invalidates the route on the outdated map, triggering a minimum-safety stop. With updates enabled, activation latency is  $1.1 \pm 0.2$  s and replanning time is  $38 \pm 6$  ms, enabling timely trajectory

refreshes.

### d) S4: Resilience under Byzantine V2X trigger injection.

We evaluate the acceptance gate under Byzantine DENM injection ( $n=10, f=3, p_{\text{attack}}=1.0$ ) while preserving a ground-truth hazard  $E^*$  that is corroborated by at least  $2f+1$  honest stations within  $(R, \tau_{\text{bft}})$  and passes the sensor veto ( $\mathcal{L}_{\text{sensor}}(E^*) \geq \eta$ ). As shown in Table V, the unfiltered V2X baseline is highly vulnerable: it accepts injected false hazards (FPR= 1.00), triggering excessive braking/replanning and collapsing route completion to 0%. In contrast, **V2X+Quorum Filter** rejects all injected false hazards (FPR= 0.00) while still accepting the true hazard (FNR= 0.00), thereby retaining the V2X safety benefit (0/30 collisions) and restoring completion to  $96.7\% \pm 2.1$ .

### e) Pareto frontier exposes controllable trade-offs and yields a stable operating point.

Figure 4 reports the measured Pareto set over  $N=60$  controller configurations, revealing a clear tracking–smoothness trade-off. We select the knee-point configuration (RMSE  $\approx 0.36$  m, smoothness  $\approx 0.72$ ) as a single operating point for S2–S4, ensuring comparisons are not confounded by hand-tuning. We quantify frontier improvement using hypervolume  $\mathcal{H}$  w.r.t. a fixed reference point  $\mathbf{r} = (1.1, 1.1, 1.1)$  on the normalized objectives ( $\tilde{J}_{\text{trk}}, \tilde{J}_{\text{sfty}}, \tilde{J}_{\text{smth}}$ ); enabling V2X increases  $\mathcal{H}$  from 0.42 (sensors-only) to 0.58 (V2X-enabled).

### f) Real-time feasibility.

Figure 5 shows the distribution of Hybrid-A\* CPU time per tick; the tail remains within the real-time budget in our scenarios.

## VII. LIMITATIONS AND CONCLUSION

### a) Conclusion.

This paper studied closed-loop motion planning and control under high-uncertainty V2X and evolving road knowledge, and presented **MORPH-U**, a CARLA-based vehicle-side stack that fuses LiDAR/radar/camera with CAM/DENM into an LDM, performs event-driven Hybrid-A\* replanning, and selects operating points via multi-objective Pareto analysis. Empirically, V2X improves closed-loop safety in hazard response (Table III), update-induced replanning restores route feasibility under knowledge changes (Table IV), and the quorum-based acceptance gate prevents false-event-induced replanning under Byzantine injection (Table V). The Pareto frontier further exposes the tracking–smoothness trade-off and supports a reproducible knee-point selection used across scenarios (Fig. 4), while planner timing remains within real-time budgets in our evaluated settings (Fig. 5).

### b) Limitations and future work.

Our evaluation is simulation-based: CARLA runs in synchronous mode, and network impairments (latency/loss/attack injection) are synthetically controlled rather than drawn from real wireless traces. Hybrid-A\*, Pure Pursuit, and PID are standard components; our contribution is a *reproducible* closed-loop methodology to quantify event-driven replanning under V2X/map updates, Pareto/knee

operating-point trade-offs, and resilience to faulty triggers. We do not yet report real-vehicle or hardware-in-the-loop (HIL) validation, and performance may shift under different sensing stacks, localization noise, or actuator limits. Our S4 evaluation covers a saturated random-injection policy; coordinated, timing-correlated, and sensor-veto-bypass attacks remain to be studied, and the gate should be regarded as Byzantine-inspired rather than formally Byzantine-tolerant. The methodological contribution—a single closed-loop stack that simultaneously exposes V2X-fusion ablations, event-driven replanning, Pareto operating-point selection, and trigger-level resilience—fills a gap left by prior work that typically isolates one or two of these axes [4], [6], [7], [29]. As next steps, we will validate MORPH-U under recorded V2X traces and HIL settings, and transfer the stack to a physical testbed.

## REFERENCES

- [1] C. Zhang, B. Tian, S. Meng, S. Qi, Y. Sun, Y. Ai, and L. Chen, “V2x-bgn: Camera-based v2x-collaborative 3d object detection with bev global non-maximum suppression,” in *2024 IEEE Intelligent Vehicles Symposium (IV)*, 2024, pp. 602–607.
- [2] Q. Delooz, A. Festag, A. Vinel, and S. C. Lobo, “Simulation-based performance optimization of v2x collective perception by adaptive object filtering,” in *2023 IEEE Intelligent Vehicles Symposium (IV)*, 2023, pp. 1–8.
- [3] S. Ribouh and A. Hadid, “Seecad: Semantic end-to-end communication for autonomous driving,” in *2024 IEEE Intelligent Vehicles Symposium (IV)*, 2024, pp. 1808–1813.
- [4] G. Kaljavesi, T. Kerbl, T. Betz, K. Mitkovskii, and F. Diermeyer, “Carla-autoware-bridge: Facilitating autonomous driving research with a unified framework for simulation and module development,” in *2024 IEEE Intelligent Vehicles Symposium (IV)*, 2024, pp. 224–229.
- [5] R. v. Kempen, L. Adrian Heidrich, B. Lampe, T. Woopen, and L. Eckstein, “Combined registration and fusion of evidential occupancy grid maps for live digital twins of traffic,” in *2023 IEEE Intelligent Vehicles Symposium (IV)*, 2023, pp. 1–6.
- [6] A. Dosovitskiy, G. Ros, F. Codevilla, A. Lopez, and V. Koltun, “CARLA: An open urban driving simulator,” in *Proceedings of the 1st Annual Conference on Robot Learning*, ser. Proceedings of Machine Learning Research, S. Levine, V. Vanhoucke, and K. Goldberg, Eds., vol. 78. PMLR, 13–15 Nov 2017, pp. 1–16. [Online]. Available: <https://proceedings.mlr.press/v78/dosovitskiy17a.html>
- [7] A. Justo, J. Araluce, J. Romera, M. Rodríguez-Arozamena, L. González, and S. Díaz, “Simbusters: Bridging simulation gaps in intelligent vehicles perception,” in *2024 IEEE Intelligent Vehicles Symposium (IV)*, 2024, pp. 2471–2476.
- [8] K. Deb, A. Pratap, S. Agarwal, and T. Meyarivan, “A fast and elitist multiobjective genetic algorithm: Nsga-ii,” *IEEE transactions on evolutionary computation*, vol. 6, no. 2, pp. 182–197, 2002.
- [9] E. Zitzler, L. Thiele, M. Laumanns, C. M. Fonseca, and V. G. da Fonseca, “Performance assessment of multiobjective optimizers: An analysis and review,” *IEEE transactions on Evolutionary Computation*, vol. 7, no. 2, pp. 117–132, 2003.
- [10] L. Lamport, R. Shostak, and M. Pease, “The byzantine generals problem,” *ACM Transactions on Programming Languages and Systems*, vol. 4, no. 3, pp. 382–401, 1982.
- [11] P. Blanchard, E. M. El Mhamdi, R. Guerraoui, and J. Stainer, “Machine learning with adversaries: Byzantine tolerant gradient descent,” in *Advances in Neural Information Processing Systems*, 2017.
- [12] C. Coue, T. Fraichard, P. Bessiere, and E. Mazer, “Multi-sensor data fusion using bayesian programming: An automotive application,” in *Intelligent Vehicle Symposium, 2002. IEEE*, vol. 2, 2002, pp. 442–447 vol.2.
- [13] W. Zhao, T. Fang, and Y. Jiang, “Data fusion using improved dempster-shafer evidence theory for vehicle detection,” in *Fourth International Conference on Fuzzy Systems and Knowledge Discovery (FSKD 2007)*, vol. 1, 2007, pp. 487–491.
- [14] S. Mentasti, A. Barbiero, and M. Matteucci, “Heterogeneous data fusion for accurate road user tracking: A distributed multi-sensor collaborative approach,” in *2024 IEEE Intelligent Vehicles Symposium (IV)*, 2024, pp. 1658–1665.
- [15] L.-C. Chen, Y. Zhu, G. Papandreou, F. Schroff, and H. Adam, “Encoder-decoder with atrous separable convolution for semantic image segmentation,” *arXiv:1802.02611*, 2018.
- [16] X. Mu, T. Qin, S. Zhang, C. Xu, and M. Yang, “Pix2planning: End-to-end planning by vision-language model for autonomous driving on carla simulator,” in *2024 IEEE Intelligent Vehicles Symposium (IV)*, 2024, pp. 2383–2390.
- [17] L. Chen, R. Lu, and X. Lin, “Blockchain-based vehicular communications: Security and privacy,” *IEEE Network*, vol. 31, no. 6, pp. 46–52, 2017.
- [18] M. Dupuis, M. Strobl, and H. Grezlikowski, “Opendrive 2010 and beyond—status and future of the de facto standard for the description of road networks,” in *Proc. of the Driving Simulation Conference Europe*, 2010, pp. 231–242.
- [19] A. Diaz-Diaz, M. Ocaña, Á. Llamazares, C. Gómez-Huélamo, P. Revenga, and L. M. Bergasa, “Hd maps: Exploiting opendrive potential for path planning and map monitoring,” in *2022 IEEE Intelligent Vehicles Symposium (IV)*, 2022, pp. 1211–1217.
- [20] F. Poggenhans, J.-H. Pauls, J. Janosovits, S. Orf, M. Naumann, F. Kuhnt, and M. Mayr, “Lanelet2: A high-definition map framework for the future of automated driving,” in *Proc. IEEE Intell. Trans. Syst. Conf.*, Hawaii, USA, November 2018. [Online]. Available: <http://www.mrt.kit.edu/z/publ/download/2018/Poggenhans2018Lanelet2.pdf>
- [21] J.-H. Pauls, T. Strauss, C. Hasberg, M. Lauer, and C. Stiller, “Hd map verification without accurate localization prior using spatio-semantic 1d signals,” in *2020 IEEE Intelligent Vehicles Symposium (IV)*, 2020, pp. 680–686.
- [22] Y. Endo, E. Javanmardi, Y. Gu, and S. Kamijo, “Evaluation of high definition map-based self-localization against occlusions in urban area,” in *2021 IEEE Intelligent Vehicles Symposium (IV)*, 2021, pp. 920–927.
- [23] C. Plachetka, N. Maier, J. Fricke, J.-A. Termöhlen, and T. Fingscheidt, “Terminology and analysis of map deviations in urban domains: Towards dependability for hd maps in automated vehicles,” in *2020 IEEE Intelligent Vehicles Symposium (IV)*, 2020, pp. 63–70.
- [24] T. Zhu, J. Leng, J. Zhong, Z. Zhang, and C. Sun, “Lanemapnet: Lane network recognition and hd map construction using curve region aware temporal bird’s-eye-view perception,” in *2024 IEEE Intelligent Vehicles Symposium (IV)*, 2024, pp. 2168–2175.
- [25] E. Bernardi, S. Masi, P. Xu, and P. Bonnifait, “High integrity lane-level occupancy estimation of road obstacles through lidar and hd map data fusion,” in *2020 IEEE Intelligent Vehicles Symposium (IV)*, 2020, pp. 1873–1878.
- [26] F. Immel, R. Fehler, M. M. Ghanaat, F. Ries, M. Hauéis, and C. Stiller, “Hd map generation from noisy multi-route vehicle fleet data on highways with expectation maximization,” in *2023 IEEE Intelligent Vehicles Symposium (IV)*, 2023, pp. 1–7.
- [27] R. Li, H. Shan, H. Jiang, J. Xiao, Y. Chang, Y. He, H. Yu, and Y. Ren, “E-mlp: Effortless online hd map construction with linear priors,” in *2024 IEEE Intelligent Vehicles Symposium (IV)*, 2024, pp. 1008–1014.
- [28] C. Gómez-Huélamo, L. M. Bergasa, R. Gutiérrez, J. F. Arango, and A. Díaz, “Smartmot: Exploiting the fusion of hdm maps and multi-object tracking for real-time scene understanding in intelligent vehicles applications,” in *2021 IEEE Intelligent Vehicles Symposium (IV)*, 2021, pp. 710–715.
- [29] C. Geller, B. Haas, A. Kloeker, J. Hermens, B. Lampe, T. Beemelmans, and L. Eckstein, “Carlos: An open, modular, and scalable simulation framework for the development and testing of software for c-its,” in *2024 IEEE Intelligent Vehicles Symposium (IV)*, 2024, pp. 3100–3106.
- [30] C. M. Elias, O. M. Shehata, E. I. Morgan, and C. Stiller, “Emerging of v2x paradigm in the development of a ros-based cooperative architecture for transportation system agents,” in *2022 IEEE Intelligent Vehicles Symposium (IV)*, 2022, pp. 1303–1308.
- [31] D. Grimm, M. Schindewolf, D. Kraus, and E. Sax, “Co-simulate no more: The carla v2x sensor,” in *2024 IEEE Intelligent Vehicles Symposium (IV)*, 2024, pp. 2429–2436.
- [32] S. Sural, N. Sahu, and R. R. Rajkumar, “Contextualfusion: Context-based multi-sensor fusion for 3d object detection in adverse operating conditions,” in *2024 IEEE Intelligent Vehicles Symposium (IV)*, 2024, pp. 1534–1541.